ACS Macro Letters

Letter

pubs.acs.org/macroletters

Design, Synthesis, and Use of Y-Shaped ATRP/NMP Surface Tethered Initiator

David R. Calabrese,[†] David Ditter,[‡] Clemens Liedel,[§] Amit Blumfield,[†] Rudolf Zentel,[‡] and Christopher K. Ober*[,§]

[†]Department of Chemistry and Chemical Biology and [§]Department of Materials Science and Engineering, Cornell University, Ithaca, New York 14853, United States

[‡]Institute of Organic Chemistry, University of Mainz, Duesbergweg 10-14, 55099 Mainz, Germany

Supporting Information

ABSTRACT: Heterogeneous polymer brushes on surfaces can be easily formed from a binary initiator on a silicon oxide substrate where two different types of polymers can be grown side-by-side. Herein, we designed a new Y-shaped binary initiator using straightforward chemistry for "grafting from" polymer brushes. This initiator synthesis takes advantage of the Passerini reaction, a multicomponent reaction combining two initiator sites and one surface linking site. This Y-shaped binary initiator can be synthesized in three steps with a higher yield than other similar initiators reported in the literature, and can be performed on a multigram scale. We were able to attach the initiator to a silicon oxide substrate and successfully grow polymer brushes from both initiators (separately and in combination), confirmed by NEXAFS, AFM, and contact angle.

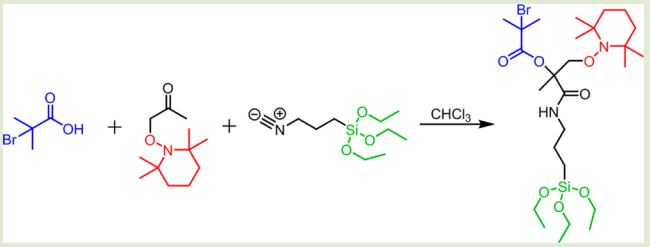

Mixed homopolymer brushes contain two or more distinct homopolymer chains that are randomly dispersed.[1−21] These mixed brush surfaces have received interest in fundamental studies and been explored in practical applications, such as "smart" surfaces, because they can form responsive surfaces.[1,22,23] When two or more types of polymer brushes are present of different polarities and there is sufficient mobility, they will rearrange themselves to minimize the brush surface energy in response to the polarity of the local environment.[1] Mixed polymer brushes, because each component segregates to form domains of similar brushes, have also been shown to form different morphologies on surfaces.[12−21,25,26] Theoretical studies have been performed on different constructions of mixed polymer brushes that indicate that desirable phase morphologies could be formed at the surface.[25]

When producing mixed homopolymer brushes, it can be quite difficult to uniformly disperse the two or more different types of polymer chains when attaching preformed chains or growing the polymer chains from well-mixed initiators.[24] This can lead to the formation of "islands" where there is a distinct zone of one type of polymer. However, using a single anchor site via a Y-shaped binary initiator, the possible difference in attachment point between the two polymers or the formation of single brush islands is eliminated.[20,22,24,27] Theoretical studies show that a Y-shaped molecule with a modest length for its "arm" should be able to create uniform mixed surfaces.[22,28,29]

Previous Y-shaped binary initiators have been synthesized by Julthongpiput and co-workers[24] and Zhao and co-workers.[13,20,27,30] Julthongpiput created a Y-shaped initiator that could be used to polymerize polystyrene (PS) on one end and poly(tert-butyl acrylate) (PtBA) on the other end.[24] At the middle point between both polymerizations was a carboxylic acid to be used to "graft to" a silicon wafer. Zhao and co-workers created a Y-shaped binary initiator with nitroxide mediated radical polymerization (NMP) and atom-transfer radical-polymerization (ATRP) initiator functions using multiple reaction steps with a trichlorosilane, dimethylchlorosilane, or triethoxysilane anchor units.[20,27,30] Such Y-shaped binary initiators can be hard to produce due to their many reaction steps and low yields. For our studies, we wished to design a Y-shaped binary initiator using a synthetic scheme that would be easier to synthesize, requiring few purification steps, produce a high yield in larger scale, and have the versatility to readily change the functionality of each arm of the initiator so that other initiator pairs could be used.

The challenging aspect to designing a Y-shaped binary initiator is that there are at least three potentially reactive functional groups that might interfere during the synthesis: a TEMPO component of the NMP initiator which reacts at high temperatures, a bromine atom that reacts with acids and metal complexes, and a silane unit that reacts with alcohols and acids. In addition to these reactive groups, other functional groups are needed to attach all of the components together. To best accomplish this combination, Passerini multicomponent chemistry was utilized.[31] Multicomponent reactions allow for

Received: March 9, 2015
Accepted: May 1, 2015
Published: May 13, 2015

DOI: 10.1021/acsmacrolett.5b00175
ACS Macro Lett. 2015, 4, 606−610

high bond forming efficiency and generally have simple experimental procedures.[32] This brings several advantages in that it allows for all three of the reactive components to be combined together in one step. If the multicomponent reaction is performed as the last step in the synthesis, then there are no intermediates with multiple reactive functional groups other than the completed initiator, which leads to fewer low yielding purification steps (Scheme 1).

Scheme 1. General Passerini Reaction

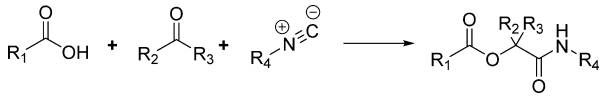

The isonitrile **3** is produced over two steps from **2** performed using methods similar to Berry and co-workers.[33] The amine is first reacted to produce a formamide by reacting with methyl formate at reflux for 24 h, which is then reduced using triphenylphosphine, carbon tetrachloride, and triethyl amine to easily produce the isonitrile in a 40% yield over two steps. The ketone (**5**) was produced in one step from TEMPO (**4**) and acetone by a gentle oxidation with $AgNO_3$ and $Na_2S_2O_8$. Utilizing the Passerini reaction, **3**, **5**, and α-bromoisobutyric acid were combined to form the binary initiator **1** with gram-scale quantities of product (Scheme 2) in a 22% overall yield in three steps (longest-linear).

Scheme 2. Synthesis of Y-Shaped Initiator

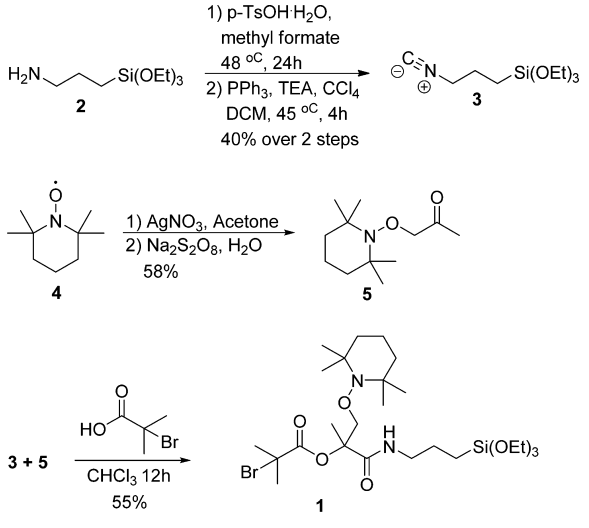

It is important to note that we selected triethoxysilane as the anchor for the Y-shaped initiator. Other ATRP initiators typically use either a mono- or trichlorosilane derivative.[13,20,27,34−37] While these initiators do have the advantage of high reactivity on silicon wafers, the reaction has to be carried out in a dried aprotic solvent, which can be difficult, to prevent unfavorable side reactions that ruin the density of the initiator attachment.[38] Conversely, trialkoxysilane groups can be attached to an oxide in the presence of water allowing for a more robust initiator.[38]

The method to attach the binary Y-shaped initiator is described and characterized in the Supporting Information. The PS growth on the surface was performed via NMP by the addition of styrene at 100 °C (Scheme 3) for 90 min. Due to the absence of any metal on the surface, ATRP could not have been carried out under these conditions. The poly(methyl methacrylate) (PMMA) growth on the surface was performed via ATRP using Cu(II)Br, with ascorbic acid added to create reducing conditions for the copper at room temperature for 2 h (Scheme 3).[39] The ATRP was carried out at room temperature to ensure that concurrent NMP reaction was not possible. NMP has been shown in similar systems to occur at temperatures of ∼80 °C or greater, which we observed as well.[13,40]

For investigating the growth of both polymerizations we studied the brush thickness after each step using ellipsometry and atomic force microscopy (AFM). Figure 1 shows a comparison of the brush thickness after NMP growth of PS and subsequent ATRP of PMMA. In Figures 1a,b, the left part of the images shows areas where the polymer was removed and the right part of each figure is intact polymer brush. Figure 1c shows the height of the AFM probe above the surface (averaged height in y-direction of Figures 1a,b; blue curve

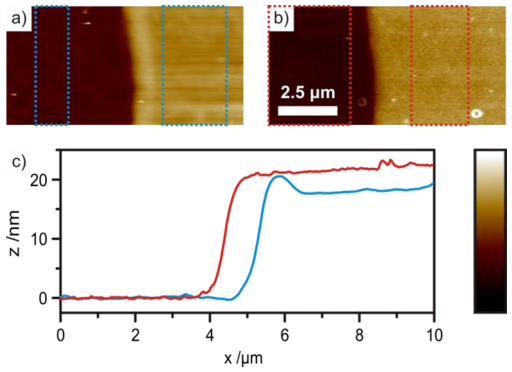

Figure 1. (a, b) AFM topography images and (c) averaged sample height of all scan lines in the y-direction (blue, height profile of a; red, height profile of b). The color bar represents a height range of 50 nm from dark to bright for (a) and (b). The scale bar corresponds to subfigures (a) and (b). The averaged vertical distance between the areas marked by blue and red dots in (a) and (b), respectively, was used to determine the film thickness.

Scheme 3. Polymerization of Polymer Brushes with Y-Shaped Initiator

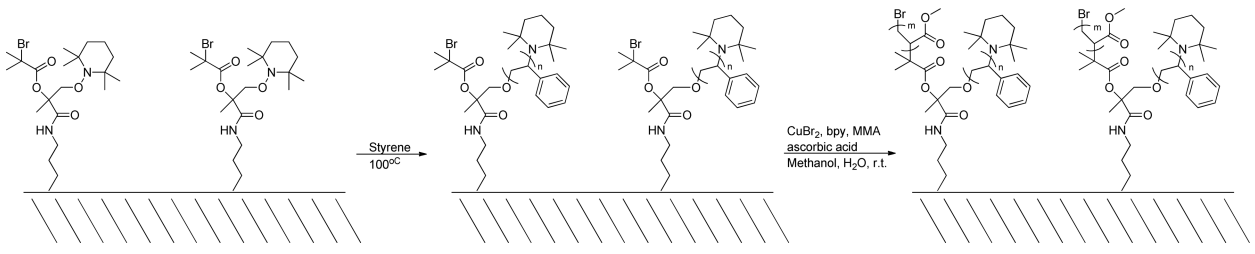

DOI: 10.1021/acsmacrolett.5b00175
ACS Macro Lett. 2015, 4, 606−610

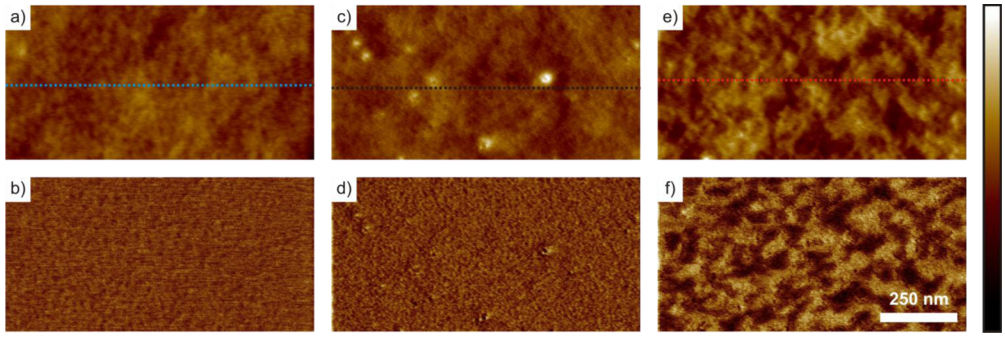

Figure 2. AFM height (a, c, e) and phase (b, d, f) images of brush samples after NMP of styrene (a, b) and after ATRP of methyl methacrylate (c and d on untreated initiator-coated surfaces, and e and f on samples where styrene brushes were grown beforehand by NMP). The color bar represents a height range of 10 nm (a, c, e) and a phase range of 5° (b, d, f) from dark to bright. The scale bar corresponds to all images. Dotted lines show the position of cross sections in Figure S2.

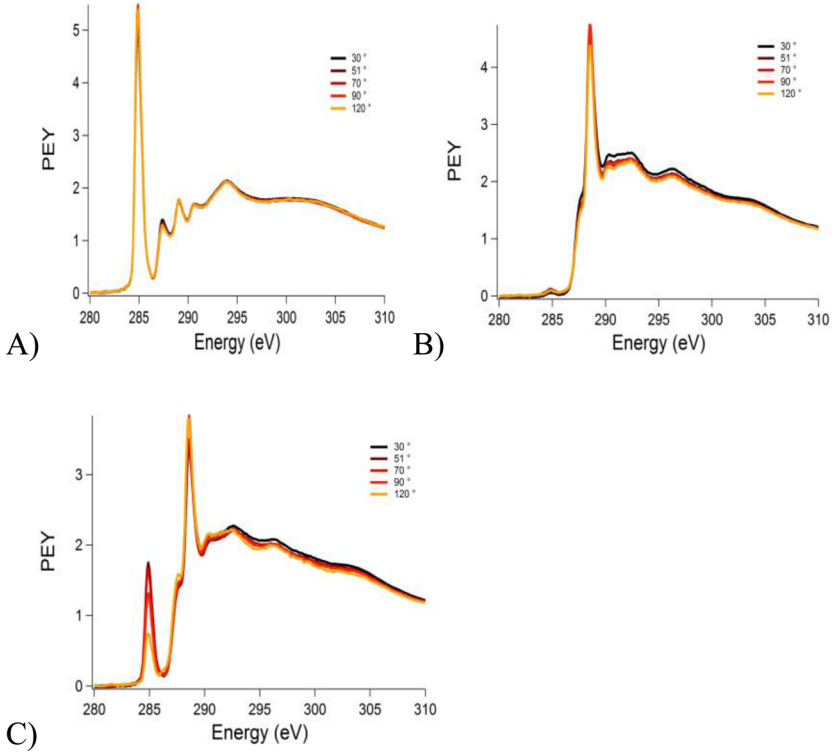

Figure 3. NEXAFS measurements of silicon wafers with (A) PS brushes, (B) PMMA brushes, and (C) PS/PMMA brushes at four different electron emission angles (30, 50, 90, and 120°).

corresponds to subfigure a, red curve to subfigure b). The height difference between the respective dotted areas in Figures 1a,b is 18.0 nm after NMP of styrene (Figure 1a) and 21.6 nm after subsequent ATRP of methyl methacrylate (Figure 1b). These values are in good agreement with ellipsometry measurements (18 and 24 nm, respectively). Brush length can be increased with increased polymerization time.

To further confirm the mixed surface composition after sequential polymerization techniques the surface topography and phase behavior of the brush surface were measured by tapping mode AFM imaging (Figure 2). Three samples were compared: we polymerized a brush of polystyrene by NMP (90 min) on the first sample and a brush of PMMA by ATRP (2 h) on the second sample, while in the third sample, ATRP of methyl methacrylate (MMA) (2 h) was performed on a sample that already contained a polystyrene brush.

The AFM phase images in Figure 2b,d,f confirms the mixed surface composition: while the phase images are almost uniformly colored, indicating a homogeneous surface composition after only NMP or only ATRP (Figure 2b,d), there are areas of two distinctly different phase values in Figure 2f (uniformly bright and uniformly dark colored areas). We note that phase contrast may not only be caused by different mechanical properties of the surface but can also by high variations in sample topography. In Figure 2f, the borders between bright and dark colored areas do not match the surface topography (Figure 2e), indicating that the phase contrast in Figure 2f is indeed a result of changes in surface composition.

Near edge X-ray absorption fine structure (NEXAFS) measurements may be used to determine both bond orientation and composition of chemical groups at the surface. Specifically, because NEXAFS spectroscopy can distinguish between aromatic carbon atoms of PS and carbonyl carbons of

DOI: 10.1021/acsmacrolett.5b00175
ACS Macro Lett. 2015, 4, 606−610

PMMA, it can be used to determine the relative concentrations of PS and PMMA at the film surfaces. The measurements at an experimental angle of 30, 50, and 90° show orientation of the brushes, while the 120° shows the population of the brushes at the top few nm.

In Figure 3A, the PS surface contains a sharp resonance peak near 285 eV which can be attributed to the C 1s → $\pi^*_{C=C}$ signal. This peak indicates the presence of aromatic carbons from the phenyl groups of PS. In Figure 3B, the PMMA surfaces contain a strong sharp resonance near 289 eV. The characteristic signals near 293 eV can be attributed to the C 1s → $\pi^*_{C=O}$ signal. The carbonyl peak is distinct to the PMMA. Figure 3A,B does not show any significant changes between the four different electronic emission angles, indicating a lack of orientation of the polymer brushes. In Figure 3C, the mixed PMMA/PS surface contains both the peak near 285 eV and the peak near 289 eV, indicating the presence of both PS and PMMA. The intensity of the peak at 289 eV is more intense than the peak at 285 eV, implying that there is more PMMA at the surface. In fact, at the most surface-sensitive angle of 120°, the peak at 285 eV is decreased, showing a reduced amount of PS at the top few nanometers of the surface. This is consistent with the AFM and ellipsometry measurements that showed that the PMMA grew longer than the PS brushes. This may further indicate the PMMA brush displacing some of the volume and pushing the PS brush up somewhat higher.

We have demonstrated the synthesis of a new Y-shaped binary initiator combining both NMP and ATRP units via simple and high yielding reactions. The initiator itself can form a uniform surface layer on a silicon oxide surface. The initiator was subsequently used to grow brushes via both ATRP and NMP. PMMA brushes could be grown through thick PS brushes already formed on the surface. We were able to demonstrate that both brush types populated the mixed brush surface using both NEXAFS, AFM, and contact angle measurements, and consistent with other studies of binary initiators that the two brushes undergo phase separation at the surface despite being grown from the same initiator. While we have not observed any regular patterns, we have noticed changes in the phase morphology at the surface. With more control of the polymer brush length, it might be possible to create regular patterns in the phase morphology.

The use of the Passerini reaction in the synthesis of the Y-shaped binary initiator provides multiple advantages including increasing the total yield of the synthesis to 22% and reducing the number of steps to three. By combining the three components at the end, it limits the amount of side reaction possible during the synthesis by limiting the number of functional groups present. The late stage addition of the three components can also allow for possible customizations of other Y-shape binary initiators.

■ ASSOCIATED CONTENT

Supporting Information

Experimental details. The Supporting Information is available free of charge on the ACS Publications website at DOI: 10.1021/acsmacrolett.5b00175.

■ AUTHOR INFORMATION

Corresponding Author

*E-mail: cko3@cornell.edu.

Notes

The authors declare no competing financial interest.

■ ACKNOWLEDGMENTS

We acknowledge support by NSF Grant DMR-1105253. This work made use of the Nanobiotechnology Center (NBTC) shared research facilities at Cornell University and the Cornell NanoScale Facility, a member of the National Nanotechnology Infrastructure Network, which is supported by the NSF (Grant ECS-0335765). We thank Dr. Edward J. Kramer, Dr. Daniel A. Fisher, and Dr. Cherno Jaye for help with NEXAFS analysis and gratefully acknowledge the use of beamline U7A at the NSLS, part of Brookhaven National Laboratories.

■ REFERENCES

(1) Horton, J. M.; Tang, S.; Bao, C.; Tang, P.; Qiu, F.; Zhu, L.; Zhao, B. *ACS Macro Lett.* **2012**, *1*, 1061−1065.
(2) Marko, J. F.; Witten, T. A. *Phys. Rev. Lett.* **1991**, *66*, 1541−1544.
(3) Zhao, B.; Zhu, L. *Macromolecules* **2009**, *42*, 9369−9383.
(4) Zhulina, E.; Balazs, A. C. *Macromolecules* **1996**, *29*, 2667−2673.
(5) Lai, P. Y. *J. Chem. Phys.* **1994**, *100*, 3351−3357.
(6) Singh, C.; Pickett, G. T.; Balazs, A. C. *Macromolecules* **1996**, *29*, 7559−7570.
(7) Sidorenko, A.; Minko, S.; Schenk-Meuser, K.; Duschner, H.; Stamm, M. *Langmuir* **1999**, *15*, 8349−8355.
(8) Minko, S.; Usov, D.; Goreshnik, E.; Stamm, M. *Macromol. Rapid Commun.* **2001**, *22*, 206−211.
(9) Lemieux, M.; Usov, D.; Minko, S.; Stamm, M.; Shulha, H.; Tsukruk, V. V. *Macromolecules* **2003**, *36*, 7244−7255.
(10) Santer, S.; Kopyshev, A.; Yang, H. K.; Rühe, J. *Macromolecules* **2006**, *39*, 3056−3064.
(11) Zhao, B. *Polymer* **2003**, *44*, 4079−4083.
(12) Zhao, B. *Langmuir* **2004**, *20*, 11748−11755.
(13) Zhao, B.; He, T. *Macromolecules* **2003**, *36*, 8599−8602.
(14) Zhao, B.; Haasch, R. T.; MacLaren, S. *J. Am. Chem. Soc.* **2004**, *126*, 6124−6134.
(15) Zhao, B.; Haasch, R. T.; MacLaren, S. *Polymer* **2004**, *45*, 7979−7988.
(16) Li, D. J.; Sheng, X.; Zhao, B. *J. Am. Chem. Soc.* **2005**, *127*, 6248−6256.
(17) Santer, S.; Kopyshev, A.; Donges, J.; Rühe, J.; Jiang, X. G.; Zhao, B.; Muller, M. *Langmuir* **2007**, *23*, 279−285.
(18) Zhao, B.; Zhu, L. *J. Am. Chem. Soc.* **2006**, *128*, 4574−4575.
(19) Zhu, L.; Zhao, B. *J. Phys. Chem. B* **2008**, *112*, 11529−11536.
(20) Jiang, X. M.; Zhong, G. J.; Horton, J. M.; Jin, N. X.; Zhu, L.; Zhao, B. *Macromolecules* **2010**, *43*, 5387−5395.
(21) Jiang, X.; Zhao, B.; Zhong, G.; Jin, N.; Horton, J. M.; Zhu, L.; Hafner, R. S.; Lodge, T. P. *Macromolecules* **2010**, *43*, 8209−8217.
(22) Julthongpiput, D.; Lin, Y.-H.; Teng, J.; Zubarev, E. R.; Tsukruk, V. V. *Langmuir* **2003**, *19*, 7832−7836.
(23) Hucknall, A.; Rangarajan, S.; Chilkoti, A. *Adv. Mater.* **2009**, *21*, 2441−2446.
(24) Wang, Z.-L.; Xu, J.-T.; Du, B.-Y.; Fan, Z.-Q. *J. Colloid Interface Sci.* **2012**, *384*, 29−37.
(25) Xue, Y. H.; Zhao, Y. W.; Fan, J. T.; Han, C.; Jiang, Z. G.; Yang, H. M.; Lui, H. *Chem. J. Chin. Univ.* **2013**, *34*, 242−248.
(26) Li, X.; Wang, M. M.; Wang, L.; Shi, X. J.; Ya, J. X.; Song, B.; Chen, H. *Langmuir* **2013**, *29*, 1122−1128.
(27) Bao, C.; Tang, S.; Horton, J. M.; Jiang, X.; Tang, P.; Qiu, F.; Zhu, L.; Zhao, B. *Macromolecules* **2012**, *45*, 8027−8036.
(28) Zhulina, E.; Balazs, A. C. *Macromolecules* **1996**, *29*, 2667.
(29) Williams, D. R. M. *J. Phys. II* **1993**, *3*, 1313.
(30) Li, W.; Bao, C.; Wright, R. A. E.; Zhao, B. *RSC Adv.* **2014**, *4*, 18772−18781.
(31) Passerini, M.; et al. *Gazz. Chim. Ital.* **1921**, *61*, 126.
(32) Dömling, A. *Chem. Rev.* **2006**, *106*, 17−89.

DOI: 10.1021/acsmacrolett.5b00175
ACS Macro Lett. 2015, 4, 606−610

(33) Berry, M.; Ramesh, K.; Champaneria, R. K.; Howell, J. A. S. *J. Mol. Catal.* **1986**, *37*, 243−252.
(34) Matyjaszewski, K.; Miller, P. J.; Shukla, N.; Immaraporn, B.; Gelman, A.; Luokala, B. B.; Siclovan, T. M.; Kickelbick, G.; Vallant, T.; Hoffmann, H.; Pakula, T. *Macromolecules* **1999**, *32*, 8716.
(35) Jeyaprakash, J. D.; Samuel, S.; Dhamodharan, R.; Rühe, J. *Macromol. Rapid Commun.* **2002**, *23*, 277.
(36) Pyun, J.; Jia, S.; Kowalewski, T.; Patterson, G. D.; Matyjaszewski, K. *Macromolecules* **2003**, *36*, 5094.
(37) Savin, D. A.; Pyun, J.; Patterson, G. D.; Kowalewski, T.; Matyjaszewski, K. *J. Polym. Sci., Part A: Polym. Chem.* **2002**, *40*, 2667.
(38) Ohno, K.; Morinaga, T.; Koh, K.; Tsujii, Y.; Fukuda, T. *Macromolecules* **2005**, *38*, 2137−2142.
(39) Min, K.; Gao, H.; Matyjaszewski, K. *Macromolecules* **2007**, *40*, 1789−1791.
(40) Becer, C. R.; Paulus, R. M.; Hoogenboom, R.; Schubert, U. S. *J. Polym. Sci., Part A: Polym. Chem.* **2006**, *44*, 6202−6213.

DOI: 10.1021/acsmacrolett.5b00175
ACS Macro Lett. 2015, 4, 606−610